CD8$^+$ T-cells control infection by exerting both cytolytic and non-cytolytic effects in different phases of the SIV lifecycle

Running head: CD8$^+$ T-cells exert both cytolytic and non-cytolytic effects on SIV infection

Supplementary Materials

Authors: B. B. Policicchio[1#], E. Fabian Cardozo-Ojeda[2#], C. Xu[3], D. Ma[3], T. He[3], K. Raehtz[4], R. Sivanandham[3], A. Kleinman[4], A. S. Perelson[5], C. Apetrei[1,4], I. Pandrea[1,3], R. M. Ribeiro[5,6]

Affiliations:
[1]Department of Infectious Diseases and Immunology, Graduate School of Public Health, University of Pittsburgh, Pittsburgh, PA, 15261 USA;
[2]Vaccine and Infectious Disease Division, Fred Hutchinson Cancer Research Center, Seattle, WA, 98109, USA;
[3]Department of Pathology, School of Medicine, University of Pittsburgh, Pittsburgh, PA, 15261, USA;
[4]Division of Infectious Diseases, Department of Medicine, School of Medicine, University of Pittsburgh, Pittsburgh, PA, 15261, USA;
[5]Theoretical Biology and Biophysics Group, Los Alamos National Laboratory, Los Alamos, NM, 87545, USA;
[6]Laboratório de Biomatemática, Faculdade de Medicina da Universidade de Lisboa, Portugal (previous address).

[#]These authors contributed equally.

Supplementary Methods

To further help interpret the viral load profiles during $CD8^+$ cell depletion and RAL monotherapy, we also used the original slow and rapid integration virus dynamic model[1] without $CD4^+$ T cell proliferation. In this case, we only fit the model to viral load observation and not to the $Ki67^+CD4^+$ T cell count. Without this assumption, the model in equation (1) in the main manuscript has the form:

$$\begin{aligned}
\frac{dT_I}{dt} &= \lambda - dT_I - \beta T_I V \\
\frac{dI_1}{dt} &= \beta T_I V - k(1-\omega)I_1 - \delta_1 I_1 \\
\frac{dM_1}{dt} &= \beta_m T_M V - k_m(1-\omega)M_1 - \delta_m M_1 \\
\frac{dI_2}{dt} &= k_m(1-\omega)M_1 + k(1-\omega)I_1 - \delta_2 I_2 \\
\frac{dV}{dt} &= pI_2 - cV
\end{aligned} \qquad \text{(S1)}.$$

To fit the model in equation S1 to the data, we used nonlinear mixed-effect modeling as described in the main text. Unlike in the main manuscript, here we only modeled the plasma viral load for animal i at time j as $y_{ij} = \log_{10} V(t_j) + \epsilon_V$ with $\epsilon_V \sim \mathcal{N}(0, \sigma_v^2)$ the error for the logged viral load.

We performed the data fitting in two steps, as this allowed better convergence of the parameter estimates. We first fitted the model in equation (S1) to the viral load data from the 8 animals under RAL monotherapy only. With this fit, we estimate parameter distributions for V_0, δ_1, δ_2, δ_m, ω and the fraction of virus produced by short-lived infected cells f_I (see [1] for model details). Other parameters were fixed as in the main text. In these initial fits, $t = 0$ refers to initiation of RAL treatment. We assumed that the system in (S1) is in steady state before $t = 0$, allowing us to obtain the values of $I_1(0) = \frac{\delta_2 c f_I V(0)}{kp}$, $M_1(0) = \frac{\delta_2 c(1-f_I)V(0)}{k_m p}$, $I_2(0) = \frac{cV(0)}{p}$, $T_I(0) = \frac{I_1(0)}{\beta V(0)}(k + \delta_1)$, $\beta_m T_M(0) = \frac{\delta_m + k_m}{V(0)} M_1(0)$ and $\lambda = \big(d + \beta V(0)\big)T_I(0)$.

In a second step, we performed fits of the model in equation (S1) to the viral load data from all 20 animals simultaneously, fixing the same parameters as before and fixing the

distribution of all parameters except $V(0)$ as estimated in the RAL-only fits. We repeat each fit by assuming that CD8$^+$ cell depletion has one or more of the following effects: (i) reduction of the death rate of short-lived infected cells before viral integration (δ_1), (ii) reduction of the death rate of productively infected cells (δ_2), (iii) increasing the viral infectivity rate (β), or (iv) increasing the virus production rate (p). These effects were simulated by changing the corresponding parameters in equation (1) under depletion conditions to $(1-\xi_1)\delta_1$, $(1-\xi_2)\delta_2$, $(1+\xi_3)\beta$ and $(1+\xi_4)p$ then estimating ξ_i, one at a time or in combination. We thus have 16 different models (Table S3), from all $\xi_i = 0$ (our original model) to all $\xi_i \neq 0$ (indicating the CD8$^+$ depletion affects each of the four parameters). Depending on the effect or combination of effects in each fit, we estimate the respective reduction or increase in each parameter (ξ_i). We fit each CD8-depletion effect model to the whole data set 10 times allowing for random initial guesses of the parameters to be estimated. Each of these times, we estimated the log-likelihood ($\log \mathcal{L}$). For the case with highest likelihood ($\max(\log \mathcal{L})$) from the 10 fits, we then computed the corrected Akaike Information Criteria (AIC) as $AIC = -2\max(\log \mathcal{L}) + 2m + \frac{2m(m+1)}{n-m-1}$, where m is the number of parameters estimated and n de number of data points from all animals[2]. We used AIC to compare models with different CD8$^+$ cell effects.

Supplementary Results

We first fitted the model to the data from the group of animals receiving RAL monotherapy only, which has also been done for HIV [3]. Virus kinetics analyses have shown that the different phases of viral decline after initiation of treatment can reveal the kinetics of infected cells [1,3]. Therefore, from these fits we aim to estimate the death rate of infected cells before (δ_1) and after integration (δ_2). These estimates will be used as reference when analyzing the effects of CD8$^+$ cell depletion. From the best fits, our model predicts that productively infected cells

have a median half-life of ~15 hrs (δ_2~1.1 day^{-1}), short-lived infected cells before integration have a median half-life of ~2.2 days (δ_1~0.31 day^{-1}), and long-lived infected cells prior integration have a median half-life of ~34 days (δ_m~0.02 day^{-1}), characterizing phases 1a, 1b and 2 of the viral decline during RAL monotherapy [1]. Also, our model also predicts that the median efficacy of RAL is 97%, except for animals RM238 and RM239 where this efficacy is 64%.

We then fitted the model to the three treatment groups together to see what effect of CD8$^+$ cell depletion best explained all the data. In this analysis, we fixed the distributions of the death rate of short-lived and long-lived infected cells before (δ_1, δ_m) and after (δ_2) integration to those estimated above with the RAL-only fits. Figure S4 show the model predictions using the median estimates of best fits to each group of animals. From the best fit, our model predicts that CD8$^+$ cell depletion affects both the loss rate of infected cells before integration (effect in δ_1) and the rate of virus production (effect in p) (ΔAIC>7 comparing to all other combinations of CD8 effects; and p=3×10^{-3} and p<1×10^{-5}, using log-likelihood ratio tests comparing to model fits assuming that CD8$^+$ depletion has effects only in *p* or only in δ_1, respectively).

Supplemental Figures

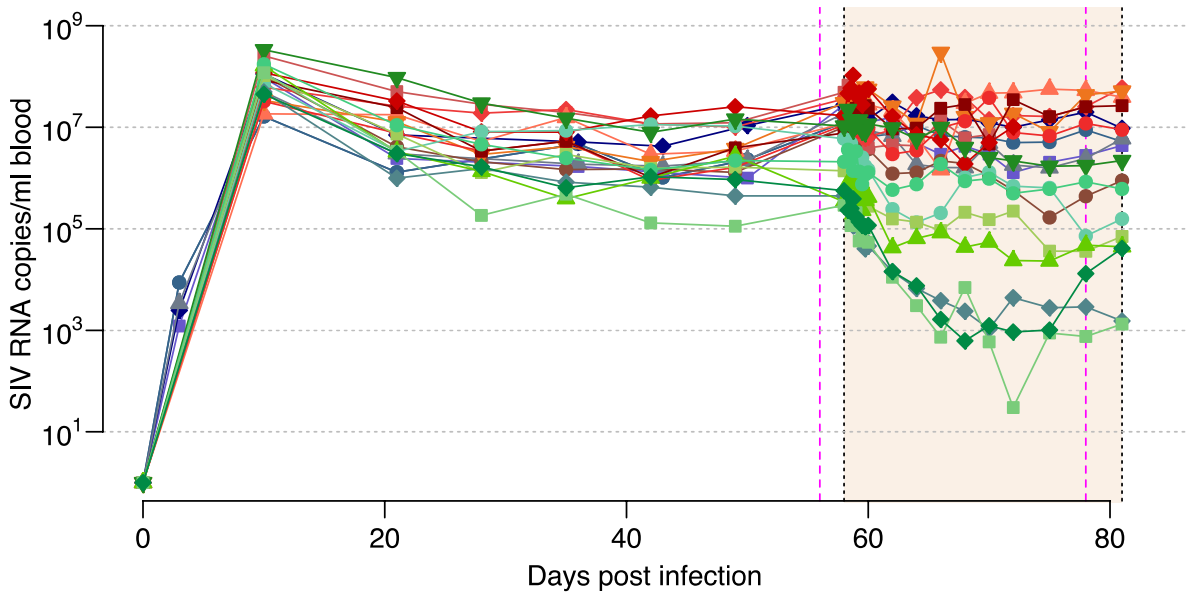

Supplemental Figure 1. Plasma viral load dynamics in all animals and treatment groups from infection to end of RAL treatment. The three treatment groups are represented with different shades of blue for CD8 depletion group, red for CD8 depletion plus RAL Tx group, and green for the RAL Tx group. Dashed magenta lines represent the times of M-T807R1 administration and the shadowed region represents RAL administration, when applicable for each group. Note that the viral load is in quasi-steady state after about 42 days post-infection.

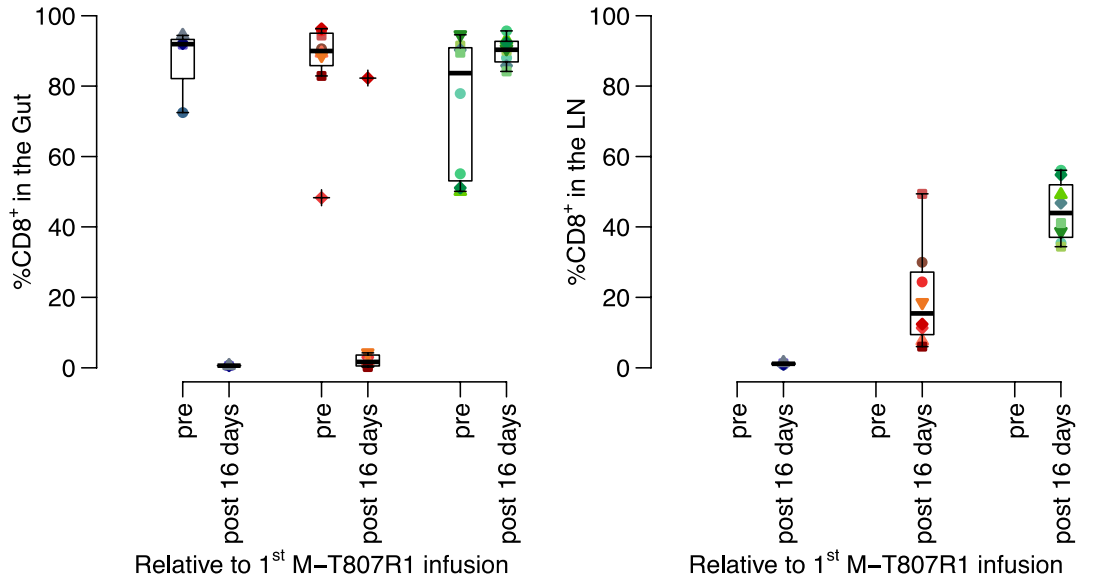

Supplemental Figure 2. The effect of M-T807R1 administration on gut and lymph node CD8⁺ T cells. %CD8⁺ T cell before the first M-T807R1 administration (after viral load has reached steady state), and 16 days after in **(left)** jejunal biopsy specimens (percentage of CD3⁺ cells) and **(right)** superficial lymph nodes (LNs) (percentage of CD3⁺ cells). For animal health reasons, we did not perform a LN biopsy sample before the CD8-cell depletion. Shades of blue: CD8 depletion group; shades of red: CD8 depletion plus RAL Tx group; and shades of green: RAL Tx group.

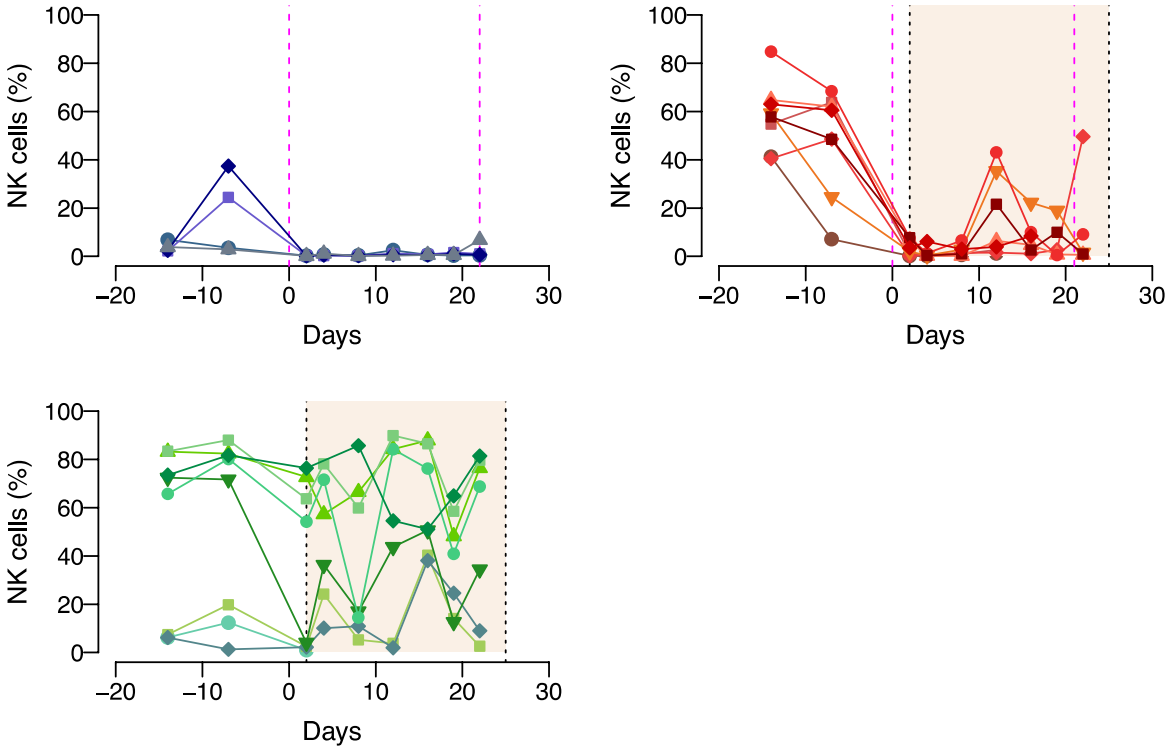

Supplemental Figure 3. The effect of M-T807R1 administrations and RAL monotherapy on peripheral NK cells. The percentage of NK cells (NKG2A^{+}) is shown for each animal in the CD8 depletion group (shades of blue); the CD8 depletion plus RAL Tx group (shades of red); and the RAL Tx group (shades of green). Dashed magenta lines represent the times of M-T807R1 administration and shadowed regions represent RAL monotherapy.

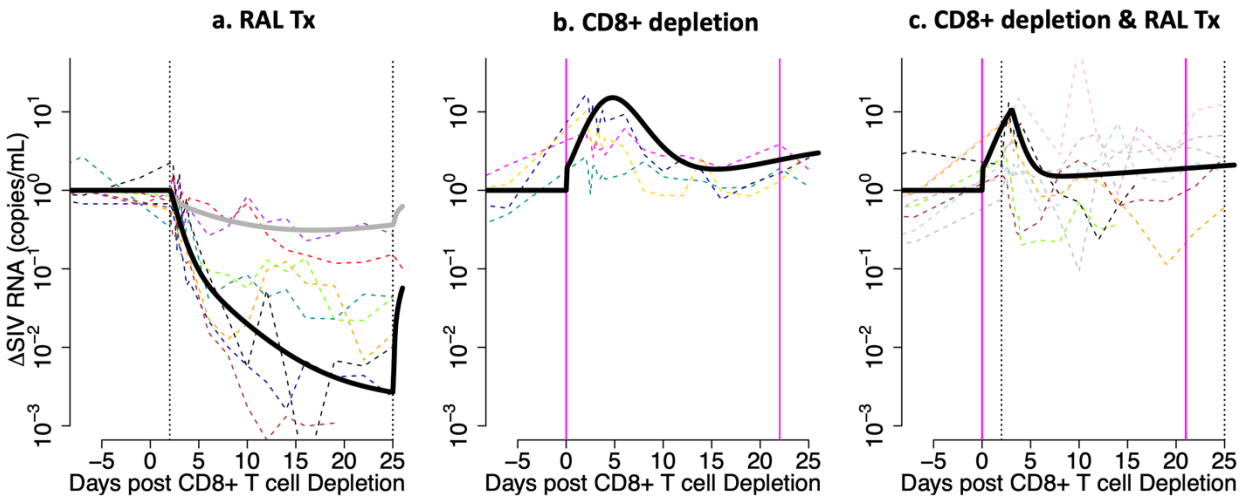

126

127 **Supplemental Figure 4. Virus dynamics fits from the alternative model of viral dynamics**
128 **developed to analyze only the observed VL data.** Population predictions for the three groups:
129 **a.** RAL Tx group; **b.** CD8 depletion group, and **c.** CD8 depletion plus RAL Tx. Vertical, dashed
130 lines represent the start and stop time of RAL monotherapy and magenta-solid lines the times of
131 M-T807R1 administration. Other colored-dashed lines represent SIV RNA copies/ml data
132 normalized to the viral load pre-intervention for each macaque. Solid, bold lines represent model
133 population predictions. Gray solid line in panel **a.** represents model predictions for animals
134 RM238 and RM239, which had a lower predicted efficacy of RAL.
135

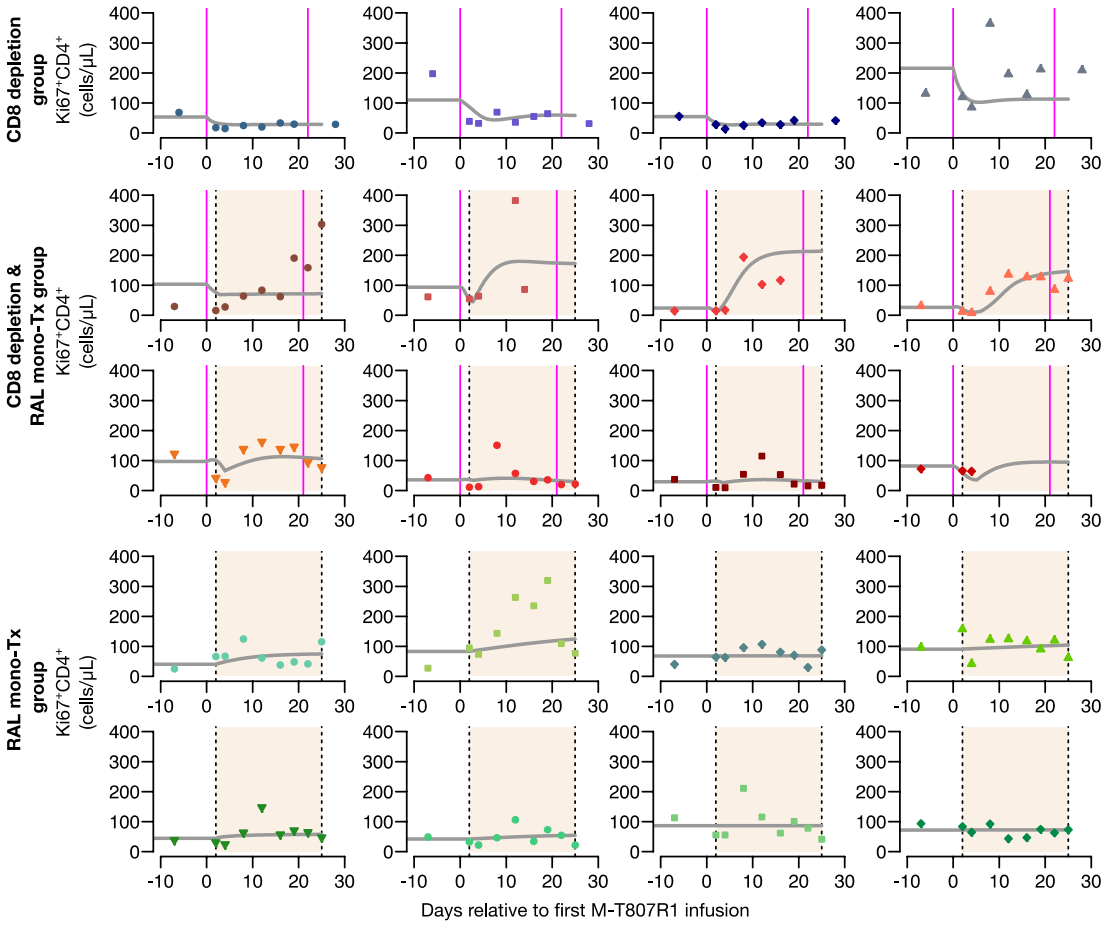

Supplemental Figure 5. Fits of the best model to the Ki67$^+$ CD4$^+$ T-cell count data. Each panel presents the dynamics of Ki67$^+$ CD4$^+$ T cells (symbols) of an individual macaque for the three study groups: CD8 depletion group (shades of blue); CD8 depletion plus RAL Tx group (shades of red); and RAL Tx group (shades of green). Magenta-solid lines represent the times of M-T807R1 administration, and the shadowed regions represent the time of RAL monotherapy. Gray solid lines in each panel represent the model fit using individual parameter estimates in Table S3.

Supplemental Tables

Supplemental Table 1. Difference in the corrected Akaike Information Criteria (ΔAICc) for the 32 model instances codifying different combinations of CD8$^+$ cell depletion effects. ΔAICc compares the AICc of a model instance with respect with the one with lowest AICc. Models with ΔAICc<5 represent the most parsimonious models (dashed blue square in the CD8$^+$ cell effect combinations). Model instances codify one of a combination of effects of CD8$^+$ cell depletion: (i) reduction of the death rate of short-lived infected cells before viral integration (δ_1), (ii) reduction of the death rate of productively infected cells (δ_2), (iii) increase in the viral infectivity rate (β), or (iv) increase in the virus production rate (p). We also allow for an effect of depletion increasing the CD4$^+$ T cell proliferation rate (r). These effects were simulated by changing the corresponding parameters in equation (1) under depletion conditions to $(1-\xi_1)\delta_1$, $(1-\xi_2)\delta_2$, $(1+\xi_3)\beta$, $(1+\xi_4)p$ and $(1+\xi_5)r$. Each row is a model instance. Green and red values per row represent ξ_i estimates significantly greater or not than zero, respectively. Gray boxes with zeros represent fixed values of ξ_i, when the respective CD8$^+$ cell effect was not considered in that model instance. This data corresponds to the one presented in Figure 5b.

	Parameters affected by CD8 depletion					#Parameters	ΔAICc
	r	p	δ_1	δ_2	β		
	ξ_5	ξ_4	ξ_1	ξ_2	ξ_3		
CD8 effect combination	3.86	0.84	0.00E+00	0.00E+00	0.00E+00	20	0.00
	4.03	0.83	1.00	0.00E+00	0.00E+00	21	0.45
	3.59	0.84	0.00E+00	2.22E-16	0.00E+00	21	1.44
	3.50	0.84	1.00	2.22E-16	0.00E+00	22	2.11
	3.85	0.84	0.00E+00	0.00E+00	2.06E-17	21	2.16
	3.99	0.88	1.00	0.00E+00	1.54E-19	22	2.39
	3.92	0.83	0.00E+00	2.22E-16	1.09E-16	22	3.96
	4.55	0.87	1.00	6.91E-14	7.40E-16	23	4.60

	6.05	0.00E+00	1.00	0.00E+00	1.34	21	7.55
	5.87	0.00E+00	0.00E+00	0.00E+00	1.42	20	7.77
	7.26	0.00E+00	1.00	0.29	0.71	22	7.89
	6.61	0.00E+00	0.00E+00	0.22	0.88	21	10.15
	7.91	0.00E+00	1.00	0.54	0.00E+00	21	11.43
	5.17	0.00E+00	0.00E+00	0.51	0.00E+00	20	13.22
	0.00E+00	0.00E+00	1.00	0.39	0.00E+00	20	15.86
	0.00E+00	0.53	1.00	2.77E-16	1.10E-15	22	18.61
	0.00E+00	0.56	1.00	0.00E+00	1.13E-16	21	19.70
	0.00E+00	0.51	1.00	2.79E-16	0.00E+00	21	22.66
	0.00E+00	0.00E+00	1.00	0.35	1.09E-16	21	22.78
	0.00E+00	0.65	1.00	0.00E+00	0.00E+00	20	24.98
	0.00E+00	0.00E+00	1.00	0.00E+00	0.68	20	29.71
	0.00E+00	0.77	0.00E+00	0.00E+00	0.00E+00	19	40.42
	0.00E+00	0.78	0.00E+00	5.14E-15	4.07E-18	21	42.34
	0.00E+00	0.77	0.00E+00	0.00E+00	5.01E-62	20	42.71
	0.00E+00	0.00E+00	0.00E+00	0.50	0.00E+00	19	43.70
	0.00E+00	0.00E+00	0.00E+00	0.50	2.51E-26	20	43.88
	0.00E+00	0.00E+00	0.00E+00	0.49	0.00E+00	20	45.21
	2.53	0.00E+00	1.00	0.00E+00	0.00E+00	20	45.97
	0.00E+00	0.00E+00	0.00E+00	0.00E+00	1.23	19	60.57
	0.00E+00	0.00E+00	1.00	0.00E+00	0.00E+00	19	84.20
	6.87	0.00E+00	0.00E+00	0.00E+00	0.00E+00	19	116.94
	0.00E+00	0.00E+00	0.00E+00	0.00E+00	0.00E+00	18	201.44

168

169

Supplemental Table 2. Difference in the corrected Akaike Information Criteria (ΔAICc) for the 16 model instances codifying different combinations of CD8⁺ cell depletion effects in the alternative model fitting only to viral loads. ΔAICc compares the AICc of a model instance with respect with the one with lowest AICc. Models with ΔAICc<5 represent the most parsimonious models (dashed blue square in the CD8⁺ cell effect combinations). Model instances codify one a combination of effects that CD8⁺ cells: (i) reduction of the death rate of short-lived infected cells before viral integration (δ_1), (ii) reduction of the death rate of productively infected cells (δ_2), (iii) increase in the viral infectivity rate (β), or (iv) increase in the virus production rate (p). These effects were simulated by changing the corresponding parameters in equation (S1) under depletion conditions to $(1-\xi_1)\delta_1$, $(1-\xi_2)\delta_2$, $(1+\xi_3)\beta$ and $(1+\xi_4)p$. Each row is a model instance. Green values per row represent ξ_i estimates significantly greater than zero. Gray boxes represent fixed values of ξ_i, when the respective CD8⁺ cell effect was not considered in that instance.

CD8 effect combination						
	Parameter affected by CD8 depletion				#Parameters	ΔAICc
	p	δ_1	δ_2	β		
	ξ_4	ξ_1	ξ_2	ξ_3		
	1.05	0.00E+00	0.00E+00	0.00E+00	11	0.00
	0.97	0.86	0.00E+00	0.00	13	3.68
	1.09	0.00E+00	0.00E+00	0.03	13	7.39
	0.80	1.00	0.05	0.00	15	7.43
	0.82	1.00	0.00E+00	0.03	15	8.76
	0.96	0.00E+00	0.04	0.00E+00	13	9.71
	0.97	0.00E+00	0.02	0.04	15	13.59
	0.00E+00	1.00	0.36	0.90	15	14.53
	0.79	1.00	0.01	0.08	17	18.99
	0.00E+00	0.00E+00	0.42	1.01	13	22.38
	0.00E+00	0.99	0.00E+00	1.34	13	22.55
	0.00E+00	0.00E+00	0.00E+00	1.37	11	44.21
	0.00E+00	0.00E+00	0.60	0.00E+00	11	48.05
	0.00E+00	0.99	0.48	0.00E+00	13	49.42
	0.00E+00	1.00	0.00E+00	0.00E+00	11	59.65
	0.00E+00	0.00E+00	0.00E+00	0.00E+00	8	205.41

Supplemental Table 3. Individual parameter estimates for the model in which CD8$^+$ cells affect death rate of infected cells prior to integration, CD4$^+$ T cell proliferation and virus production. For all animals the population estimates for the CD8+ cell effects were: $\xi_1 = 1$, $\xi_4 = 0.83$ and $\xi_5 = 4$.

	ID	f_I	$\log_{10} V_0$	r	K	δ_1	δ_2	δ_m	ω	$\log_{10} \beta$	p	τ
CD8 depletion	**RM126**	0.97	6.4	0.04	15.2	0.15	1.4	0.02	-	-7.8	39718	-
	RM128	0.97	6.2	0.01	25.8	0.15	2.6	0.02	-	-7.8	39943	-
	RM129	0.97	6.8	0.03	17.0	0.15	1.4	0.02	-	-7.8	39361	-
	RM130	0.97	6.3	0.01	27.9	0.13	3.8	0.02	-	-7.8	25474	-
CD8 depletion & RAL	**RM123**	0.97	6.3	0.04	46.0	0.15	1.8	0.02	0.94	-7.8	28286	0.9
	RM124	0.97	7.1	0.03	102.6	0.15	2.5	0.02	0.95	-7.6	28289	0.8
	RM194	0.96	7.1	0.07	256.9	0.14	2.0	0.02	0.95	-7.2	36274	0.5
	RM233	0.96	6.8	0.06	286.4	0.14	1.4	0.02	0.93	-7.4	29991	4.0
	RM234	0.97	6.6	0.04	193.3	0.15	1.4	0.02	0.94	-8.0	33003	2.0
	RM235	0.97	6.3	0.02	77.2	0.15	1.0	0.02	0.93	-7.8	36633	0.9
	RM236	0.97	6.4	0.03	82.9	0.15	1.0	0.02	0.93	-7.8	51423	1.6
	RM178	0.96	7.1	0.02	53.8	0.14	1.3	0.02	0.94	-7.9	32152	3.1
RAL	**RM193**	0.96	6.9	0.03	21.4	0.13	1.4	0.02	0.95	-7.7	43746	1.2
	RM125	0.97	6.3	0.02	95.2	0.14	1.7	0.02	0.94	-7.8	27851	1.2
	RM196	0.95	5.8	0.05	5.4	0.15	2.3	0.02	0.94	-7.7	44692	1.2
	RM195	0.96	6.0	0.02	102.2	0.12	1.1	0.02	0.95	-8.0	26483	1.2
	RM238	0.97	7.2	0.04	7.2	0.15	0.9	0.02	0.77	-7.8	36839	1.2
	RM239	0.96	6.4	0.03	28.8	0.15	1.2	0.02	0.78	-7.8	39506	1.2
	RM240	0.97	5.4	0.06	2.9	0.15	1.1	0.02	0.95	-7.9	33539	1.2
	RM179	0.97	5.8	0.05	4.3	0.15	1.5	0.02	0.95	-7.8	38230	1.2

References

1. Cardozo, E.F.*, et al.* Treatment with integrase inhibitor suggests a new interpretation of HIV RNA decay curves that reveals a subset of cells with slow integration. *PLoS Pathog* **13**, e1006478 (2017).
2. Burnham, K. & Anderson, D. *Model Selection and Multimodel Inference*, (Springer, New York, New York, 2004).
3. Andrade, A.*, et al.* Early HIV RNA decay during raltegravir-containing regimens exhibits two distinct subphases (1a and 1b). *AIDS (London, England)* **29**, 2419-2426 (2015).